Improvement of the memory quality of optical pulse pairs in atomic systems via four-wave mixing

Datang Xu,[1,2] Chao Hang,[1,3] and Guoxiang Huang[1,3]
[1]*State Key Laboratory of Precision Spectroscopy, East China Normal University, Shanghai 200062, China*
[2]*School of Physics and Electronic Engineering, Changshu Institute of Technology, Changshu 215500, China*
[3]*NYU-ECNU Joint Institute of Physics at NYU-Shanghai, Shanghai 200062, China*

(Received 20 August 2018; published 25 October 2018)

We present a scheme to improve the memory quality of linear and nonlinear optical pulse pairs via four-wave mixing (FWM) in an atomic gas. We show that in a linear regime the efficiency and fidelity of the memory of the probe and Stokes pulses can be largely improved through an elimination of the fast-light mode (and hence the suppression of the optical gain induced by the FWM process). We also show that in a nonlinear regime the system may support stable optical soliton pairs with ultraslow propagation velocity and ultralow generation power, which can also be stored and retrieved with a better quality. The improved optical pulse pair memory suggested here may have promising applications in optical information processing and transformation.

DOI: 10.1103/PhysRevA.98.043848

I. INTRODUCTION

In recent years, much attention has been paid to the study of slow lights via electromagnetically induced transparency (EIT), a typical quantum interference effect occurring in three-level Λ-type atomic systems interacting resonantly with two (i.e., probe and control) laser fields [1,2]. One of the most important applications of EIT is optical pulse memory, a very useful technique for optical information processing and communication networks [3–6]. Based on dark-state polariton inherent in EIT systems, the probe field can be mapped into an atomic mode, stored temporarily, and then retrieved from the atomic mode through switching off and on of the control laser field [7–11].

EIT-based schemes for optical pulse memory are not necessarily restricted to three-level Λ-type atomic systems. One typical example is the generalization to a four-level system with a double-Λ-type configuration. In an early work, Zibrov *et al.* [12] showed that transporting and multiplexing of stored light is possible in a double-Λ system. Later, many interesting studies on optical memory using double-Λ systems (or their variants) were carried out both theoretically and experimentally, aiming to find new characters for the optical memory that are absent in three-level systems, especially for realizing pulse pair memories and even multimode memories [13–22]. However, the FWM process in double-Λ systems brings an optical gain to both Stokes and probe fields, and hence lowers the quality of the optical memory. Generally, such optical gain is unavoidable for large optical depth, and thus with double-Λ systems it is very difficult to realize an optical memory with high efficiency and fidelity [23].

In this work, we present a scheme to improve the memory quality of linear and nonlinear optical pulse pairs via the four-wave mixing (FWM) process in a cold atomic gas with a double-Λ-type level configuration. First, in the linear regime we show that generally both probe and Stokes pulses co-propagating in the system contain simultaneously two normal modes, i.e., slow-light and fast-light modes, and the existence of the fast-light mode severely lowers the memory quality of both pulses. By suppressing the fast-light mode (and thereby the optical gain to both Stokes and probe fields induced by the FWM process) under a suitable physical condition, we found that a significant improvement of the efficiency and fidelity of the memory of the probe and Stokes pulses is realizable. Then, we generalize our theoretical approach to a weak nonlinear regime, and demonstrate that the system may support stable optical soliton pairs, which have ultraslow propagation velocity and ultralow generation power. These optical soliton pairs can also be stored and retrieved with better efficiency and fidelity than that of linear optical pulse pairs. The improvement scheme for the memory quality of optical pulse pairs suggested here may have promising applications in optical information processing and transformation.

The remainder of the paper is arranged as follows. Section II gives a description of the model under study. Section III presents the result on stable linear optical pulse pairs and investigates their storage and retrieval. Section IV demonstrates that stable optical soliton pairs and their storage and retrieval are possible in the system. Finally, Sec. V summarizes the main results obtained in this work.

II. MODEL

We start by considering a cold gas consisting of four-state atoms with double-Λ-type level configuration, shown in Fig. 1(a). States $|1\rangle$ and $|2\rangle$ are hyperfine splitting of atomic ground state and $|3\rangle$ and $|4\rangle$ are two excited states. The atoms are assumed to be initially prepared in the ground state $|1\rangle$. A weak, pulsed probe laser field (with center angular frequency ω_p and wave number k_p) couples the transition $|1\rangle \leftrightarrow |3\rangle$, while another weak, pulsed Stokes field (with center angular frequency ω_s and wave number k_s) couples the transition $|2\rangle \leftrightarrow |4\rangle$ [24]. In addition, two strong, continuous-wave control laser fields, i.e., control field 1 (with center angular frequency ω_{c1} and wave number k_{c1}) and control field 2 (with center angular frequency ω_{c2} and wave number k_{c2}), couple the transitions $|1\rangle \leftrightarrow |4\rangle$

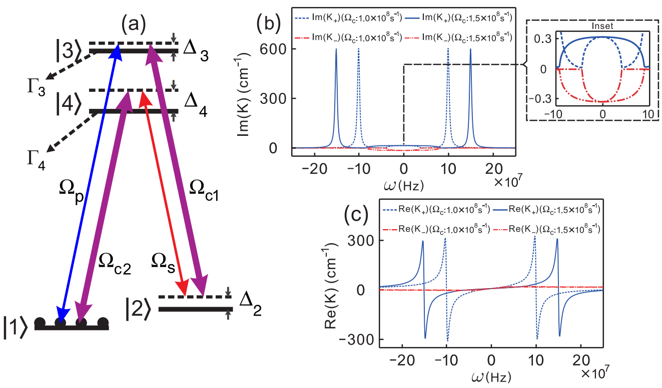

FIG. 1. (a) Energy-level diagram and excitation scheme of the double-Λ system. Ω_p and Ω_s (Ω_{c1} and Ω_{c2}) are respectively half Rabi frequencies of the probe and Stokes fields (control field 1 and control field 2); Δ_j ($j = 2, 3, 4$) are detunings; Γ_3 and Γ_4 are respectively decay rates of the levels $|3\rangle$ and $|4\rangle$. Black dots mean that the population is initially prepared at the state $|1\rangle$. For light propagation the system has two eigenmodes, i.e., slow-light and fast-light modes, which are collective (normal) modes of the system with linear dispersion relations respectively given by K_+ and K_-. (b) Im($K_\pm$) as functions of ω [25] for $\Delta_2 = \Delta_3 = 0$ and $\Delta_4 = 0.5$ GHz. The dashed (solid) blue line is for $\Omega_{c1} = \Omega_{c2} \equiv \Omega_c = 1.0 \times 10^8$ Hz (1.5×10^8 Hz); dashed-dotted (dashed-dotted-dotted) red line is for K_- mode for $\Omega_c = 1.0 \times 10^8$ Hz (1.5×10^8 Hz). The inset shows the detail of Im($K_\pm$) near $\omega = 0$. (c) Re($K_\pm$) as functions of ω. K_+ is an absorptive (slow-light) mode, whereas K_- is a gain (fast-light) mode which contributes to the FWM gain in the optical memory (see text for more detail).

and $|2\rangle \leftrightarrow |3\rangle$, respectively. The total electric field in the system can be expressed as $\mathbf{E} = \mathbf{E}_{c1} + \mathbf{E}_p + \mathbf{E}_{c2} + \mathbf{E}_s = \sum_{l=c1,p,c2,s} \mathbf{e}_l \mathcal{E}_l \exp[i(k_l z - \omega_l t)] + \text{c.c.}$, where $\mathbf{e}_l$ ($\mathcal{E}_l$) are the unit polarization vectors (envelopes) of the electric field $\mathbf{E}_l$. For simplicity, we have assumed that all laser fields propagate along the z direction.

Under electric-dipole and rotating-wave approximations, the Hamiltonian of the system in the interaction picture is given by

$$\hat{H}_{\text{int}} = -\hbar \sum_{j=2}^{4} \Delta_j |j\rangle\langle j| - \hbar[\Omega_{c1}|3\rangle\langle 2| + \Omega_p|3\rangle\langle 1| + \Omega_{c2}|4\rangle\langle 1| + \Omega_s|4\rangle\langle 2| + \text{H.c.}], \tag{1}$$

where Ω_p, Ω_s, Ω_{c1}, and Ω_{c2} are respectively half Rabi frequencies of the probe field, Stokes field, control field 1, and control field 2, defined by $\Omega_p = (\boldsymbol{p}_{31} \cdot \mathbf{e}_p)\mathcal{E}_p/\hbar$, $\Omega_s = (\boldsymbol{p}_{42} \cdot \mathbf{e}_s)\mathcal{E}_s/\hbar$, $\Omega_{c1} = (\boldsymbol{p}_{32} \cdot \mathbf{e}_{c1})\mathcal{E}_{c1}/\hbar$, and $\Omega_{c2} = (\boldsymbol{p}_{41} \cdot \mathbf{e}_{c2})\mathcal{E}_{c2}/\hbar$, respectively. Here $\boldsymbol{p}_{jl}$ is the electric-dipole matrix element associated with the transition $|j\rangle \leftrightarrow |l\rangle$; $\Delta_2 = \omega_{c2} - \omega_s - (E_2 - E_1)/\hbar = \omega_p - \omega_{c1} - (E_2 - E_1)/\hbar$, $\Delta_3 = \omega_p - (E_3 - E_1)/\hbar$, and $\Delta_4 = \omega_{c2} - (E_4 - E_1)/\hbar$ are detunings, with E_j the eigenenergy of the state $|j\rangle$.

The motion of the atoms is governed by the optical Bloch equation, given by

$$i\hbar\left(\frac{\partial}{\partial t} + \Gamma\right)\sigma = [\hat{H}_{\text{int}}, \sigma], \tag{2}$$

where σ is a 4×4 density matrix describing the atomic population and coherence and Γ is a 4×4 relaxation matrix describing the spontaneous emission and dephasing of the system. The explicit expression of Eq. (2) is given in Appendix A.

The propagation of the probe and the Stokes fields is governed by the Maxwell equation, which under the slowly varying envelope approximation is given by

$$i\left(\frac{\partial}{\partial z} + \frac{1}{c}\frac{\partial}{\partial t}\right)\Omega_p(z,t) + \kappa_{13}\,\sigma_{31}(z,t) = 0, \tag{3a}$$

$$i\left(\frac{\partial}{\partial z} + \frac{1}{c}\frac{\partial}{\partial t}\right)\Omega_s(z,t) + \kappa_{24}\,\sigma_{42}(z,t) = 0. \tag{3b}$$

Here $\kappa_{13} = \mathcal{N}_a\omega_p|\mathbf{p}_{13}|^2/(2\varepsilon_0 c\hbar)$ and $\kappa_{24} = \mathcal{N}_a\omega_s|\mathbf{p}_{24}|^2/(2\varepsilon_0 c\hbar)$ are coupling constants, with c the light speed in vacuum and $\mathcal{N}_a$ the atomic density.

Note that when deriving the above Maxwell-Bloch (MB) equations (2) and (3), the following assumptions have been made: (i) The probe and Stokes pulses have large transverse sizes so that the diffraction effect of the system is negligible. (ii) Both control fields are strong enough, so that their half Rabi frequencies, i.e., Ω_{c1} and Ω_{c2}, can be taken to be undepleted during the evolution of the probe and Stokes pulses. However, when considering the storage and retrieval of the probe and Stokes pulses, Ω_{c1} and Ω_{c2} will be assumed to be changed slowly in time. (iii) The atomic gas is cold enough and dilute enough, so that thee Doppler effect is negligible and the interaction between atoms can be described by the dephasing parameter γ_{jl}^{dep} (see Appendix A). (iv) In general, phases of the four laser fields may play a role in the FWM process; however, here for simplicity we assume they are zero (i.e., all four Rabi frequencies are real). (v) Generally, the FWM effect makes both the Stokes and probe fields acquire not only the optical gain discussed in this work but also a production of quantum (or vacuum) noise [23]. In our work, we limit our study to the suppression of the optical gain. We consider the case that the photon numbers in both the Stokes and probe fields are large, and hence the quantum noise in the system is negligible. In this situation, a semiclassical approach to the system can be exploited.

III. STORAGE AND RETRIEVAL OF LINEAR OPTICAL PULSES

A. Linear dispersion relation

The base-state solution (i.e., the steady-state solution when the probe and the Stokes fields are absent) of the MB Eqs. (2) and (3) is given by $\sigma_{11}^{(0)} = (1 + \frac{|d_{41}|^2}{|\Omega_{c2}|^2})\sigma_{44}^{(0)}$, $\sigma_{22}^{(0)} = \frac{\Gamma_{24}}{\Gamma_{13}}(1 + \frac{|d_{32}|^2}{|\Omega_{c1}|^2})\sigma_{44}^{(0)}$, $\sigma_{33}^{(0)} = \frac{\Gamma_{24}}{\Gamma_{13}}\sigma_{44}^{(0)}$, $\sigma_{32}^{(0)} = -\frac{\Gamma_{24}}{\Gamma_{13}}\frac{d_{32}^*}{\Omega_{c1}^*}\sigma_{44}^{(0)}$, and $\sigma_{41}^{(0)} = -\frac{d_{41}^*}{\Omega_{c2}^*}\sigma_{44}^{(0)}$, where $\sigma_{44}^{(0)} = 1/[2 + \Gamma_{24}(2 + |d_{32}|^2/|\Omega_{c1}|^2)/\Gamma_{13} + |d_{41}|^2/|\Omega_{c2}|^2]$. If Δ_4 is large, the base-state solution is simplified to $\sigma_{11}^{(0)} \approx 1$ with all other density matrix elements nearly zero.

When weak probe and Stokes fields are applied, the system undergoes a linear evolution. In this case, the MB Eqs. (2) and (3) can be solved through a Fourier transform, with the general solution given by

$$\Omega_p(z,t) = \int_{-\infty}^{\infty} d\omega [F_p^{+}(\omega) e^{i\theta_+} + F_p^{-}(\omega) e^{i\theta_-}], \tag{4a}$$

$$\Omega_s^*(z,t) = \int_{-\infty}^{\infty} d\omega [G_+(\omega) F_p^{+}(\omega) e^{i\theta_+} + G_-(\omega) F_p^{-}(\omega) e^{i\theta_-}], \tag{4b}$$

where $\theta_\pm = K_\pm z - \omega t$ [25] and $G_\pm = (K_\pm - \omega/c - \delta_{11})/\delta_{12}$. Here F_p^+ and F_p^- are transform amplitudes, depending on the boundary condition of the probe and Stokes fields [i.e., $\Omega_p(0,t)$ and $\Omega_s(0,t)$], see Eq. (6) below.

In the above expressions, K_+ and K_- are linear dispersion relations of the system, which read

$$K_\pm(\omega) = \frac{\omega}{c} + \tfrac{1}{2}[(\delta_{11} - \delta_{22}) \pm \sqrt{(\delta_{11} - \delta_{22})^2 - 4(\delta_{12}\delta_{21} - \delta_{11}\delta_{22})}], \tag{5}$$

where $\delta_{11} = \kappa_{13}(\alpha_{11}\sigma_{33}^{(0)} + \beta_{21}\sigma_{11}^{(0)})$, $\delta_{12} = \kappa_{13}(\alpha_{12}\sigma_{32}^{(0)} + \beta_{22}\sigma_{41}^{(0)})$, $\delta_{21} = \kappa_{24}(\alpha_{21}\sigma_{32}^{(0)*} + \beta_{11}\sigma_{41}^{(0)*})$ and $\delta_{22} = \kappa_{24}(\alpha_{22}\sigma_{22}^{(0)} + \beta_{12}\sigma_{44}^{(0)})$, with explicit expressions of $\alpha_{ij}(\omega)$ and $\beta_{ij}(\omega)$ presented in Appendix B. We see that the linear dispersion relations have two branches, which means that the system allows two eigenmodes, i.e., K_+ and K_- modes. Since both the probe and the Stokes pulses are linear superpositions of these two modes (or inversely each mode is a particular linear composition of the probe and Stokes pulses), K_+ and K_- modes have a character of collective excitations and hence can be called normal modes of the system. Note that in our scheme $\mathbf{p}_{13} \approx \mathbf{p}_{24}$ and $\kappa_{13} = \kappa_{24}$, thus the linear optical susceptibility of the system is given by $\chi_\pm = \frac{\mathcal{N}_a|\mathbf{p}_{13}|^2}{\epsilon_0\hbar}\frac{K_\pm}{\kappa_{13}}$.

Shown in Fig. 1(b) is the imaginary parts of the linear dispersion relation, i.e., $\mathrm{Im}[K_\pm(\omega)]$, as functions of ω. When plotting the figure, we have chosen a cold alkali ^{87}Rb atomic gas, with atomic levels assigned as $|1\rangle = |5^2S_{1/2}, F=1, m_F=0\rangle$, $|2\rangle = |5^2S_{1/2}, F=2, m_F=0\rangle$, $|3\rangle = |5^2P_{3/2}, F=2, m_F=1\rangle$ and $|4\rangle = |5^2P_{3/2}, F=2, m_F=-1\rangle$. The system parameters are $\Gamma_{12} = 5\times10^3$ Hz, $\Gamma_{13} = \Gamma_{23} = 5\times10^6$ Hz, $\Gamma_{14} = \Gamma_{24} = 3\times10^6$ Hz, $\Delta_2 = \Delta_3 = 0$, $\Delta_4 = 10$ GHz, $\kappa_{13} = \kappa_{24} = 1.8\times10^{10}$ cm^{-1}s^{-1}, and $\mathcal{N}_a = 3.3\times10^{11}$ cm^{-3} [18,19,21,26]. In the figure, the dashed (solid) blue line is for the K_+ mode for $\Omega_{c1} = \Omega_{c2} \equiv \Omega_c = 1.0\times10^8$ Hz $(1.5\times10^8$ Hz), the dashed-dotted (dashed-dotted-dotted) red line is for the K_- mode for $\Omega_c = 1.0\times10^8$ Hz $(1.5\times10^8$ Hz). The inset illustrates the detail of $\mathrm{Im}(K_\pm)$ near $\omega = 0$. Shown in Fig. 1(c) is the real part of $K_\pm$, i.e., $\mathrm{Re}(K_\pm)$.

From Fig. 1(b), we see that the K_+ mode is an absorptive one [because $\mathrm{Im}(K_+) > 0$]; in addition, a transparency window is opened in the profile of $\mathrm{Im}(K_+)$, which becomes wider when the control fields are increased. From Fig. 1(c), we see that the group velocity (given by $[\partial\mathrm{Re}(K_+)/\partial\omega]^{-1}$) near $\omega = 0$ is positive and less than c (subluminal), hence the K_+ mode is a slow-light mode [27]. On the contrary, $\mathrm{Im}(K_-)$ is negative [see the inset of Fig. 1(b)], thus the K_- mode is a gain mode. Since the group velocity of the K_- mode is larger than c and even can be negative (superluminal), it is a fast-light mode. It is just this fast-light mode that results in an optical gain to both the probe and Stokes fields, and thereby lowers the quality of the propagation and memory of the probe and Stokes pulses in the double-Λ system, see below.

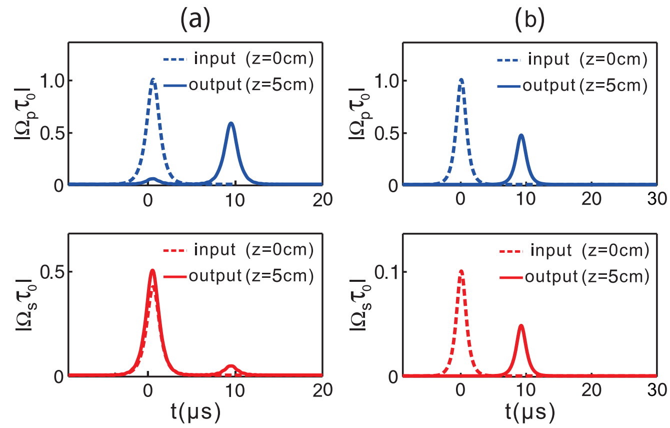

FIG. 2. Propagation of linear probe pulse (blue) and Stokes pulse (red). In each panel, the upper (lower) part is for the probe (Stokes) field, with the dashed line for the input (at $z=0$) and solid line for the output (at $z=5$ cm). (a) Propagation without the suppression of the K_- mode. In this case, the probe and Stokes pulses contain both the slow- and fast-light modes, and a large deformation occurs during propagation. (b) Propagation with the suppression of the K_- mode. In this case, both the probe and Stokes pulses contain only the slow-light mode and thus can keep their wave shapes during propagation (except for some decay due to the absorption of the slow-light mode).

B. Suppression of the fast-light mode

To confirm the above analytical conclusion, a numerical simulation on the linear propagation of both probe and Stokes pulses is carried out. Shown in Fig. 2(a) is the result of the propagation of the probe pulse (blue color) and the Stokes pulse (red color) as functions of time. The upper (lower) part is for the probe (Stokes) pulse, with the dashed line for the input (at $z=0$) and solid line for the output (at $z=5$ cm). The boundary condition (at $z=0$) used is $\Omega_{p0}(t)\tau_0 = \mathrm{sech}(1.5t/\tau_0)$ and $\Omega_{s0}(t)\tau_0 = 0.5\,\mathrm{sech}(1.5t/\tau_0)$. System parameters are $\Omega_{c1} = \Omega_{c2} = 1.0\times10^8$ Hz, $\tau_0 = 1.0\times10^{-6}$ s, $\Delta_2 = 10$ MHz, $\Delta_3 = 0$, and $\Delta_4 = 10$ GHz, with other ones the same as those used in Fig. 1(b). We see that both the probe and Stokes pulses have indeed a significant deformation (especially for the Stokes pulse) during propagation. The reason is that both of them contain the slow-light (K_+) mode and the fast-light (K_-) mode (which can be clearly seen by the two peaks in the output pulses shown in the figure). Consequently, to realize a stable propagation (and also memory) of both pulses, one must eliminate the fast-light mode in the system.

We now make an analysis for how to suppress the fast-light mode. From Eq. (4) we obtain

$$F_p^+ = \frac{-G_-}{G_+ - G_-}\tilde{\Omega}_p + \frac{1}{G_+ - G_-}\tilde{\Omega}_s^*, \tag{6a}$$

$$F_p^- = \frac{G_+}{G_+ - G_-}\tilde{\Omega}_p - \frac{1}{G_+ - G_-}\tilde{\Omega}_s^*, \tag{6b}$$

with $\tilde{\Omega}_p \equiv \tilde{\Omega}_p(z,\omega)|_{z=0} = \frac{1}{2\pi}\int dt\,\Omega_p(0,t)e^{i\omega t}$ and $\tilde{\Omega}_s \equiv \tilde{\Omega}_s(z,\omega)|_{z=0} = \frac{1}{2\pi}\int dt\,\Omega_s(0,t)e^{-i\omega t}$. To eliminate the fast-light (K_-) mode, one should suppress the value of F_p^- to zero, which, obviously, can be realized if the condition

$$\tilde{\Omega}_s^*(z,\omega)|_{z=0} = G_+(\omega)\tilde{\Omega}_p(z,\omega)|_{z=0} \tag{7}$$

can be satisfied.

Shown in Fig. 2(b) is the propagation of the probe and Stokes pulses when condition (7) is fulfilled. The boundary condition (at $z=0$) is chosen as $\Omega_{p0}(t)\tau_0 = \mathrm{sech}(1.5t/\tau_0)$ but $\Omega_{s0}^*(t) = \mathcal{F}^{-1}[G_+\tilde{\Omega}_{p0}]$, where $\mathcal{F}^{-1}$ means an inverse Fourier transform. The system parameters used here are $\tau_0 = 1.0\times10^{-6}$ s, $\Omega_{c10}=\Omega_{c20}=1.0\times10^8$ Hz, $\Delta_2 = 10$ MHz, $\Delta_3=0$, and $\Delta_4 = 10$ GHz. We see that both the probe and Stokes pulses have nearly the same wave shapes and can keep the wave shapes during propagation. The reason is that in the present situation both probe and Stokes pulses contain only the slow-light mode, and they have a common, ultraslow group velocity V_g (it is approximately $1.78\times10^{-5}c$ with the system parameters given in the figure), except for some decay in their amplitudes. Note that when plotting Figs. 2(a) and 2(b), a nonzero Δ_2 is chosen, which is to suppress the dephasing effect between the two lower levels $|1\rangle$ and $|2\rangle$ (i.e., γ_{21}).

To fulfill condition (7), one must prepare the system with a particular Stokes field at the input boundary $z=0$, i.e., the seeded idler (i.e., the Stokes field) at the entrance of the medium should be specially designed. Such design of the seeded idler can be realized through a preparation of the input Stokes pulse based on the properties of the system [including the dispersion feature of $K_+(\omega)$ mode since $G_+(\omega)$ is proportional to $K_+(\omega)$] [28].

C. Storage and retrieval of linear pulse pairs

Now we turn to considering the memory of linear probe and Stokes pulses in the double-Λ system. To implement the memory, it is needed to manipulate the two control fields Ω_{c1} and Ω_{c2}. Their switching off and on can be modeled by the combination of two hyperbolic tangent functions of the form [29]

$$\Omega_{cj} = \Omega_{c0j}\left\{1-\frac{1}{2}\tanh\left[\frac{t-T_{\rm off}}{T_s}\right]+\frac{1}{2}\tanh\left[\frac{t-T_{\rm on}}{T_s}\right]\right\}, \tag{8}$$

where Ω_{c0j} $(j=1,2)$ are constants, $T_{\rm off}$ and $T_{\rm on}$ are respectively times of switching off and switching on, and T_s is switching time. The storage time of the probe and the Stokes pulses is given by $T_{\rm on}-T_{\rm off}$. The efficiency of the optical memory for optical pulse l $(l=p,s)$ can be characterized by [30]

$$\eta_l = \frac{\int_{-\infty}^{T_{\rm off}}|\Omega_l^{\rm in}(t)|^2dt - \left|\int_{-\infty}^{T_{\rm off}}|\Omega_l^{\rm in}(t)|^2dt - \int_{T_{\rm on}}^{+\infty}|\Omega_l^{\rm out}(t)|^2dt\right|}{\int_{-\infty}^{T_{\rm off}}|\Omega_l^{\rm in}(t)|^2dt}. \tag{9}$$

The fidelity of the memory is characterized by $\eta_l J_l^2$, with

$$J_l^2 = \frac{\left|\int_{-\infty}^{T_{\rm off}}\Omega_l^{\rm out}(t)\Omega_l^{\rm in}(t+\Delta T)dt\right|^2}{\int_{-\infty}^{T_{\rm off}}|\Omega_l^{\rm out}(t)|^2dt\int_{T_{\rm on}}^{\infty}|\Omega_l^{\rm in}(t)|^2dt}, \tag{10}$$

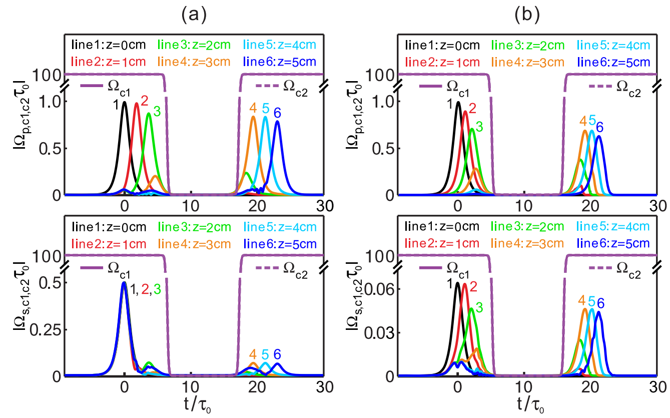

FIG. 3. Storage and retrieval of linear optical pulse pair. (a) The case without suppression of the fast-light (K_-) mode. The upper (lower) part is the result of the memory of the probe (Stokes) pulse. In each part, lines 1 to 6 are for the pulse propagating to $z=0,1,2,3,4,$ and 5 cm, respectively. The solid and dashed magenta lines are curves of $|\Omega_{c1}\tau_0|$ and $|\Omega_{c2}\tau_0|$, respectively; they (when overlapped completely) represent the switching off and on of the two control fields. In this case the Stokes pulse has a bad retrieval [lower part of (a)]. (b) The same as (a) but with suppression of the fast-light mode. In this case the memory efficiency and fidelity of the Stokes pulse is improved greatly compared with the case in (a) where the fast-light mode is not suppressed.

where $\Omega_l^{\rm in}(t) = \Omega_l(z,t)|_{z=0}$, $\Omega_l^{\rm out}(t)=\Omega_l(z,t)|_{z=L_z}$ (L_z is the length of the medium), and ΔT is the time interval between the peak of the input pulse and that of the retrieved pulse.

A numerical simulation is carried out on the storage and retrieval of both the probe and Stokes pulses, based on solving the MB Eqs. (2) and (3). Figure 3(a) shows the result of the simulation in the presence of the fast-light (K_-) mode. The boundary condition (at $z=0$) used is $\Omega_{p0}(t)\tau_0 = \mathrm{sech}(1.5t/\tau_0)$ and $\Omega_{s0}(t)\tau_0 = 0.5\,\mathrm{sech}(1.5t/\tau_0)$ [24], and system parameters are chosen as $T_s=\tau_0$, $T_{\rm off}=5\,\tau_0$ and $T_{\rm on}=18\,\tau_0$, $\tau_0=1.0\times10^{-6}$ s, $\Omega_{c10}=\Omega_{c20}=1.0\times10^8$ Hz, $\Delta_2=10$ MHz, $\Delta_3=0$, and $\Delta_4=10$ GHz. In the figure, the upper (lower) part is the memory result of the probe (Stokes) pulse. In each part, lines 1 to 6 are for the pulse propagating to $z=0$, 1, 2, 3, 4, and 5 cm, respectively. The solid (dashed) magenta line represents the switching off and on of control field 1 (control field 2); they overlap completely since we have taken $\Omega_{c1}=\Omega_{c2}$. The memory efficiency and fidelity of the probe (Stokes) pulse are found to be $\eta_p = 62.84\%$ and $\eta_p J_p^2 = 62.47\%$ ($\eta_s = 2.17\%$ and $\eta_s J_s^2 = 2.10\%$), respectively. As expected, in this case the Stokes pulse has a bad memory quality because it contains the fast-light mode (i.e., the FWM gain).

Shown in Fig. 3(b) is the result of the simulation on both the optical pulses with the suppression of the fast-light (K_-) mode. To suppress the fast-light mode, the boundary condition (at $z=0$) is chosen as $\Omega_{p0}(t)\tau_0=\mathrm{sech}(1.5t/\tau_0)$ but $\Omega_{s0}^*(t)=\mathcal{F}^{-1}[G_+\tilde{\Omega}_{p0}]$. In addition, For eliminating the significant dispersion effect that exists for linear pulses, we choose $\Delta_2 = 1.3\times10^7$ Hz without changing other system parameters. From the figure we obtain that the memory efficiency and fidelity of the probe (Stokes) pulse are respectively given by $\eta_p = 52.11\%$ and $\eta_p J_p^2 = 50.55\%$ ($\eta_s = 45.38\%$ and $\eta_s J_s^2 = 44.50$). We see that in this case the memory efficiency and fidelity of the Stokes pulse is improved greatly compared with the case without the suppression of the FWM gain [the case of Fig. 3(a)], although the memory quality of the probe pulse has a small decrease.

IV. STORAGE AND RETRIEVAL OF OPTICAL SOLITONS

The results presented above are valid only for linear optical pulses. Now we generalize our approach to a weak nonlinear optical regime. It is well known that linear pulses usually suffer a spreading due to the existence of dispersion, which may result in a serious distortion of optical pulses. For practical applications, it is desirable to obtain optical pulses that are robust during the processes of propagation and memory. One way to realize this is to employ the Kerr nonlinearity to balance the dispersion in the system. Recent studies have shown that ultraslow optical solitons are possible in EIT systems [31,32] and they can also be stored and retrieved [33,34].

A. Ultraslow optical soliton pairs

To obtain possible weak-light soliton pairs in the present system, we employ the approach developed in Ref. [32]. Nonlinearly coupled envelope equations describing the evolution of the probe and Stokes pulses can be derived from the MB Eqs. (2) and (3) by using a method of multiple scales, which read

$$i\left(\frac{\partial}{\partial z}+\alpha_+\right)U^+ - \frac{K_2^+}{2}\frac{\partial^2 U^+}{\partial \tau^2} - (W_{11}|U^+|^2 + W_{12}|U^-|^2)U^+ = 0, \tag{11a}$$

$$i\left(\frac{\partial}{\partial z}+\alpha_-\right)U^- - \frac{K_2^-}{2}\frac{\partial^2 U^-}{\partial \tau^2} - (W_{21}|U^+|^2 + W_{22}|U^-|^2)U^- = 0, \tag{11b}$$

where $\tau = t - z/V_g$ ($V_g \approx V_g^+$), $U^+ = F_p^+ e^{-\alpha_+ z}$, $U^- = F_p^- e^{-\alpha_- z}$ ($\alpha_\pm = \epsilon^{-2}\mathrm{Im}[K_\pm]$), and $K_2^\pm = \partial^2 K_\pm/\partial\omega^2$ describe second-order dispersions, and W_{11} and W_{22} (W_{12} and W_{21}) are coefficients of self-phase modulation (cross-phase modulation). Explicit expressions of W_{lm} ($l, m = 1, 2$) are presented in Appendix C.

To suppress the fast-light mode and hence the optical gain due to the FWM, we assume that the system works under condition (7), and hence U^- can be neglected. In this situation, only Eq. (11a) preserves; its solution can be easily obtained. Then we have the probe and Stokes solitons with forms

$$\Omega_p(z,t) = \frac{1}{\tau_p}\sqrt{\frac{\tilde{K}_2^+}{\tilde{W}_{11}}}\,\mathrm{sech}\left[\frac{1}{\tau_p}\left(t-\frac{z}{\tilde{V}_g^+}\right)\right]e^{i[\tilde{K}_0-1/(2L_D)]z}, \tag{12a}$$

$$\Omega_s(z,t) = \frac{G_+(0)}{\tau_p}\sqrt{\frac{\tilde{K}_2^+}{\tilde{W}_{11}}}\,\mathrm{sech}\left[\frac{1}{\tau_p}\left(t-\frac{z}{\tilde{V}_g^+}\right)\right]e^{i[\tilde{K}_0-1/(2L_D)]z}, \tag{12b}$$

where $K_0 = K_+(\omega)|_{\omega=0}$, and $G_+(0) = G_+(\omega)|_{\omega=0}$. The tilde means the real part of the quantity, i.e., $\tilde{K}_2^+ = \mathrm{Re}(K_2^+)|_{\omega=0}$ and $\tilde{W}_{11} = \mathrm{Re}(W_{11})|_{\omega=0}$. We call Eqs. (12a) and (12b) the optical soliton pair of the system.

By taking a set of realistic system parameters $\Omega_{c1} = \Omega_{c2} = 1.0\times10^8$ Hz, $\tau_0 = 1.0\times10^{-6}$ s, $\Delta_2 = 1.0\times10^7$ Hz, $\Delta_3 = 2.3\times10^8$ Hz, $\kappa_{23} = 2.4\times10^{10}$ cm^{-1} Hz, and $\mathcal{N}_a = 4.35\times10^{11}$ cm^{-3}, we obtain $K_0 = 19.57 + 0.08i$ cm^{-1} and $\tilde{K}_2^+ = (9.86 + 0.33i)\times10^{-15}$ cm^{-1} s^2. To get a Kerr nonlinearity that can balance the dispersion of the system, we choose $|\Omega_{p,\max}|\tau_0 = 12$ (here $\Omega_{p,\max}$ is the maximum amplitude of Ω_p). Then we have $\tilde{W}_{11} = (1.55\times10^{-14} - 0.8\times10^{-17}i)$ cm^{-1} s^2. We see that imaginary parts of K_0, $\tilde{K}_2^+$, and $\tilde{W}_{11}$ are much smaller than their real parts, which is due to the EIT effect induced by the two control fields. With these results we obtain $\mathrm{Re}(V_g^+) \approx 1.28\times10^{-5}\,c$. Thereby, both the probe and Stokes solitons travel with a common, ultraslow propagating velocity. The result means that the optical soliton pair is quite robust during propagation thanks to the suppression of the fast-light mode.

The light power for generating such an optical soliton pair can be calculated by using the Poynting vector integrated over the cross section S_0 of the optical pulses [32]. By taking $S_0 = 1.0$ mm^2, we obtain the maximum light power for generating such optical soliton pairs, given by $P_{\max} \approx 2.2\,\mu$W, which is very low compared with that of the optical solitons produced in other optical media (such as optical fibers).

B. Storage and retrieval of the optical soliton pairs

Lastly, we investigate the storage and retrieval of the ultraslow optical soliton pair predicted above. To this end, we solve the MB Eqs. (2) and (3) numerically by assuming that both control fields Ω_{c1} and Ω_{c2} to be switched off and on according to the form given by the expression (8). In the numerical simulation, we take $T_s = 1.0\tau_0$, $T_{\rm off} = 5.0\tau_0$, and $T_{\rm on} = 18.0\tau_0$, with other parameters the same as those used in Fig. 3.

Shown in Fig. 4 are results of the storage and retrieval of the ultraslow optical soliton pair. Figure 4(a) is for the evolution of $|\Omega_p\tau_0|$, i.e., for the probe soliton component, as a function of time t for different propagation distances z. Lines 1 to 6 in each panel are for $z = 0$, 1, 2, 3, 4, and 5 cm, respectively. The solid and dashed purple lines are curves of $|\Omega_{c1}\tau_0|$ and $|\Omega_{c2}\tau_0|$, respectively; they (when overlapped completely) represent the switching off and on of the two control fields. Figure 4(b) is similar to Fig. 4(a), but for $|\Omega_s\tau_0|$, i.e., the Stokes soliton component. In the simulation, the input condition of the probe pulse at $z = 0$ is taken as $\Omega_{p0}(t)\tau_0 = 12\,\mathrm{sech}(1.5t/\tau_0)$, while the input condition of the Stokes field is taken as $\mathcal{F}^{-1}[G_+\tilde{\Omega}_{p0}]$, i.e., fulfilling condition (7) for suppressing the FWM gain.

From the figure we see that because of the balance between the dispersion and the nonlinearity, the probe and the Stokes pulses suffer less deformation (spreading) than the linear case

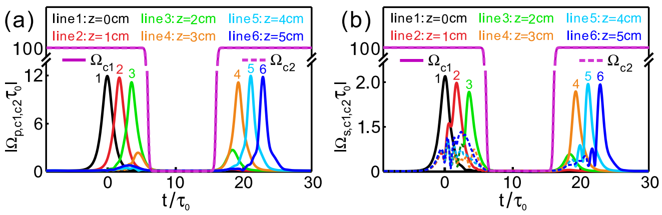

FIG. 4. Storage and retrieval of the ultraslow optical soliton pair. (a) Evolution of $|\Omega_p\tau_0|$ for the probe soliton component as a function of time t for different propagation distance z. Lines 1 to 6 are for the soliton propagating to $z = 0$, 1, 2, 3, 4, and 5 cm, respectively; the solid and dashed purple lines are curves of $|\Omega_{c1}\tau_0|$ and $|\Omega_{c2}\tau_0|$, respectively; they (when overlapped completely) represent the switching off and on of the two control fields. (b) The same as (a) but for $|\Omega_s\tau_0|$, i.e., the Stokes soliton component.

(Fig. 3) during the propagation. When both control fields are switched off at $t = T_{\rm off} = 5.0\tau_0$, both components of the soliton pair disappear, and then they appear again when both control fields are switched on again at $t = T_{\rm on} = 18.0\tau_0$ [35]. In this nonlinear regime, the memory efficiencies of the probe and Stokes components reach respectively $\eta_p = 67.62\%$ and $\eta_s = 61.91\%$, which is an increase of 16% compared with the one in the linear regime. The memory fidelity of the probe (Stokes) component reaches $\eta_p J_p^2 = 64.73\%$ ($\eta_s J_s^2 = 56.71\%$), which also is an increase of 14% (12%) compared with the one in the linear regime. Thus the memory of the ultraslow optical soliton pair has a better quality than that of the linear optical pulse pair shown in the last section due to the suppression of the dispersion by the Kerr nonlinearity of the system.

V. SUMMARY

In this work, we have proposed a scheme for improving the memory quality of optical pulse pairs via FWM in a cold, double-Λ atomic gas. We have shown that in general both the probe and Stokes pulses contain a slow-light mode and a fast-light mode that copropagate in the system simultaneously; the existence of the fast-light mode may severely lower the memory quality of both pulses. By suppressing the fast mode (and thereby the optical gain induced by the FWM effect) under a suitable condition, we found that a significant improvement of the efficiency and fidelity of the memory of the probe and Stokes pulses is realizable. We have also shown that the system may support ultraslow optical soliton pairs through the balance between the dispersion and the Kerr nonlinearity in the system. The ultraslow, weak-light soliton pairs can also be stored and retried with better efficiency and fidelity than that of linear optical pulse pairs.

Our work on the optical memory in the double-Λ system can be generalized to many other cases, including the memory of high-dimensional linear and nonlinear optical pulse pairs carrying with orbital angular momenta the phase control of the optical memory, the design of slow-light routers, the extension to an all-quantum approach, etc. Thus the improvement scheme for optical pulse pair memory suggested here has promising applications in all-optical information processing and transformation.

ACKNOWLEDGMENTS

This work was supported by National Natural Science Foundation of China under Grants No. 11475063 and No. 11474099, and by National Basic Research Program of China under Grant No. 2016YFA0302103.

APPENDIX A: EXPLICIT EXPRESSIONS OF THE BLOCH EQUATION AND THEIR SIMPLIFIED FORM

The explicit expression of the optical Bloch equation reads [36]

$$i\frac{\partial}{\partial t}\sigma_{11} - i\Gamma_{13}\sigma_{33} - i\Gamma_{14}\sigma_{44} + \Omega_p^*\sigma_{31} + \Omega_{c2}^*\sigma_{41} - \Omega_p\sigma_{31}^* - \Omega_{c2}\sigma_{41}^* = 0, \tag{A1a}$$

$$i\frac{\partial}{\partial t}\sigma_{22} - i\Gamma_{23}\sigma_{33} - i\Gamma_{24}\sigma_{44} + \Omega_{c1}^*\sigma_{32} + \Omega_s^*\sigma_{42} - \Omega_{c1}\sigma_{32}^* - \Omega_s\sigma_{42}^* = 0, \tag{A1b}$$

$$i\left(\frac{\partial}{\partial t} + \Gamma_3\right)\sigma_{33} + \Omega_p\sigma_{31}^* + \Omega_{c1}\sigma_{32}^* - \Omega_p^*\sigma_{31} - \Omega_{c1}^*\sigma_{32} = 0, \tag{A1c}$$

$$i\left(\frac{\partial}{\partial t} + \Gamma_4\right)\sigma_{44} + \Omega_{c2}\sigma_{41}^* + \Omega_s\sigma_{42}^* - \Omega_{c2}^*\sigma_{41} - \Omega_s^*\sigma_{42} = 0, \tag{A1d}$$

for diagonal matrix elements, and

$$\left(i\frac{\partial}{\partial t} + d_{21}\right)\sigma_{21} + \Omega_{c1}^*\sigma_{31} + \Omega_s^*\sigma_{41} - \Omega_p\sigma_{32}^* - \Omega_{c2}\sigma_{42}^* = 0, \tag{A2a}$$

$$\left(i\frac{\partial}{\partial t} + d_{31}\right)\sigma_{31} + \Omega_p(\sigma_{11} - \sigma_{33}) + \Omega_{c1}\sigma_{21} - \Omega_{c2}\sigma_{43}^* = 0, \tag{A2b}$$

$$\left(i\frac{\partial}{\partial t} + d_{32}\right)\sigma_{32} + \Omega_{c1}(\sigma_{22} - \sigma_{33}) + \Omega_p\sigma_{21}^* - \Omega_s\sigma_{43}^* = 0, \tag{A2c}$$

$$\left(i\frac{\partial}{\partial t} + d_{41}\right)\sigma_{41} + \Omega_{c2}(\sigma_{11} - \sigma_{44}) + \Omega_s\sigma_{21} - \Omega_p\sigma_{43} = 0, \tag{A2d}$$

$$\left(i\frac{\partial}{\partial t}+d_{42}\right)\sigma_{42}+\Omega_s(\sigma_{22}-\sigma_{44})+\Omega_{c2}\sigma_{21}^*-\Omega_{c1}\sigma_{43}=0, \tag{A2e}$$

$$\left(i\frac{\partial}{\partial t}+d_{43}\right)\sigma_{43}+\Omega_{c2}\sigma_{31}^*+\Omega_s\sigma_{32}^*-\Omega_p^*\sigma_{41}-\Omega_{c1}^*\sigma_{42}=0, \tag{A2f}$$

for nondiagonal matrix elements. Here $d_{21}=\Delta_2+i\gamma_{21}$, $d_{31}=\Delta_3+i\gamma_{13}$, $d_{32}=\Delta_3-\Delta_2+i\gamma_{23}$, $d_{41}=\Delta_4+i\gamma_{14}$, $d_{42}=\Delta_4-\Delta_2+i\gamma_{24}$, $d_{43}=\Delta_4-\Delta_3+i\gamma_{34}$, $\gamma_{ij}=(\Gamma_i+\Gamma_j)/2+\gamma_{ij}^{\mathrm{dep}}$, and $\Gamma_j=\sum_{i<j}\Gamma_{ij}$, with Γ_{ij} the spontaneous emission decay rate and $\gamma_{ij}^{\mathrm{dep}}$ the dephasing rate between state $|i\rangle$ and state $|j\rangle$ [36].

APPENDIX B: DEFINITIONS OF $\alpha_{ij}(\omega)$ AND $\beta_{ij}(\omega)$

The explicit expression of $\alpha_{ij}(\omega)$ and $\beta_{ij}(\omega)$ in Eq. (5) reads

$$\begin{aligned}
\alpha_{11}(\omega)&=\frac{\omega+d_{41}^*}{|\Omega_{c2}|^2-\omega(\omega+d_{41}^*)}, & \alpha_{12}(\omega)&=\frac{-\Omega_{c2}}{|\Omega_{c2}|^2-\omega(\omega+d_{41}^*)},\\
\alpha_{21}(\omega)&=\frac{-\Omega_{c2}^*}{|\Omega_{c2}|^2-\omega(\omega+d_{41}^*)}, & \alpha_{22}(\omega)&=\frac{\omega}{|\Omega_{c2}|^2-\omega(\omega+d_{41}^*)},\\
\beta_{11}(\omega)&=\frac{-\Omega_{c1}^*}{|\Omega_{c1}|^2-(\omega+d_{21})(\omega+d_{31})}, & \beta_{12}(\omega)&=\frac{\omega+d_{31}}{|\Omega_{c1}|^2-(\omega+d_{21})(\omega+d_{31})},\\
\beta_{21}(\omega)&=\frac{\omega+d_{21}}{|\Omega_{c1}|^2-(\omega+d_{21})(\omega+d_{31})}, & \beta_{22}(\omega)&=\frac{-\Omega_{c1}}{|\Omega_{c1}|^2-(\omega+d_{21})(\omega+d_{31})}.
\end{aligned} \tag{B1}$$

APPENDIX C: EXPLICIT EXPRESSIONS OF THE COEFFICIENTS IN EQS. (11)

The coefficients in Eqs. (11) are written into a matrix form for simplicity:

$$W_{11}=[W_{11}'+W_{12}'|G_+|^2+W_{21}'G_++W_{22}'G_+|G_+|^2], \tag{C1a}$$

$$W_{21}=[2W_{11}'+W_{12}'G_+^*(G_++G_-)+W_{21}'(G_++G_-)+W_{22}'(G_++G_-)|G_+|^2], \tag{C1b}$$

$$W_{12}=[2W_{11}'+W_{12}'G_-^*(G_++G_-)+W_{21}'(G_++G_-)+W_{22}'(G_++G_-)|G_-|^2], \tag{C1c}$$

$$W_{22}=[W_{11}'+W_{12}'|G_-|^2+W_{21}'G_-+W_{22}'G_-|G_-|^2], \tag{C1d}$$

where the expressions for W_{11}', W_{12}', W_{21}', W_{22}' are

$$\begin{aligned}W_{21}'=\big[&\alpha_{11}^2\beta_{11}^*\sigma_{33}^{(0)}+\alpha_{11}\alpha_{12}\beta_{21}^*\sigma_{32}^{(0)}+\alpha_{11}^*\beta_{21}\beta_{22}\sigma_{43}^{(0)}+\alpha_{21}^*\beta_{21}\beta_{22}\sigma_{31}^{(0)*}\\&+\alpha_{12}\beta_{21}\beta_{11}^*\sigma_{11}^{(0)}+\alpha_{11}\beta_{22}\beta_{21}^*\sigma_{41}^{(0)}+\alpha_{11}^*\alpha_{12}\beta_{21}\sigma_{32}^{(0)}+\alpha_{11}\alpha_{21}^*\beta_{22}\sigma_{33}^{(0)}\big],\end{aligned} \tag{C2a}$$

$$\begin{aligned}W_{12}'=\big[&\alpha_{12}\alpha_{21}\beta_{12}^*\sigma_{33}^{(0)}+\alpha_{11}\alpha_{22}\beta_{22}^*\sigma_{32}^{(0)}+\alpha_{12}^*\beta_{12}\beta_{21}\sigma_{43}^{(0)}+\alpha_{22}^*\beta_{11}\beta_{22}\sigma_{31}^{(0)*}\\&+\alpha_{12}\beta_{21}\beta_{12}^*\sigma_{41}^{(0)*}+\alpha_{11}|\beta_{22}|^2\sigma_{44}^{(0)}+|\alpha_{12}|^2\beta_{21}\sigma_{22}^{(0)}+\alpha_{11}\alpha_{22}^*\beta_{22}\sigma_{32}^{(0)*}\big],\end{aligned} \tag{C2b}$$

$$W_{22}'=\big[\alpha_{12}\alpha_{22}\beta_{12}^*\sigma_{32}^{(0)}+\alpha_{22}^*\beta_{22}\beta_{12}\sigma_{43}^{(0)}+\alpha_{12}\beta_{22}\beta_{12}^*\sigma_{44}^{(0)}+\alpha_{12}\alpha_{22}^*\beta_{22}\sigma_{22}^{(0)}\big], \tag{C2c}$$

$$W_{11}'=\big[\alpha_{11}^2\beta_{21}^*\sigma_{33}^{(0)}+\alpha_{11}^*\beta_{21}^2\sigma_{31}^{(0)*}+\alpha_{11}|\beta_{21}|^2\sigma_{11}^{(0)}+|\alpha_{11}|^2\beta_{21}\sigma_{33}^{(0)}\big]. \tag{C2d}$$

[1] M. Fleischhauer, A. Imamoglu, and J. P. Marangos, Electromagnetically induced transparency: Optics in coherent media, Rev. Mod. Phys. **77**, 633 (2005).

[2] *Slow Light: Science and Applications*, edited by J. B. Khurgin and R. S. Tucker (CRC Press, Boca Raton, FL, 2009).

[3] A. I. Lvovsky, B. C. Sanders, and W. Tittel, Optical quantum memory, Nat. Photon. **3**, 706 (2009).

[4] C. Simon, M. Afzelius, J. Appe, A. B. Giroday, S. J. Dewhurst, N. Gisin, C. Hu, F. Jelezko, S. Kröll, J. Müler, J. Nunn, E. Polzik, J. Rarity, H. Riedmatten, W. Rosenfeld, A. J. Shields, N. Sköld, R. M. Stevenson, R. Thew, I. Walmsley, M. Weber, H. Weinfurter, J. Wrachtrup, and R. J. Young, Quantum memories, Eur. Phys. J. D **58**, 1 (2010).

[5] N. Sangouard, C. Simon, H. de Riedmatten, and N. Gisin, Quantum repeaters based on atomic ensembles and linear optics, Rev. Mod. Phys. **83**, 33 (2011).

[6] F. Bussières, N. Sangouarda, M. Afzeliusa, H. de Riedmattenb, C. Simon, and W. Tittel, Prospective applications of optical quantum memories, J. Mod. Opt. **60**, 1519 (2013).

[7] M. Fleischhauer and M. D. Lukin, Dark-State Polaritons in Electromagnetically Induced Transparency, Phys. Rev. Lett. **84**, 5094 (2000).

[8] C. Liu, Z. Dutton, C. H. Behroozi, and L. V. Hau, Observation of coherent optical information storage in an atomic medium using halted light pulses, Nature **409**, 490 (2001).

[9] M. D. Eisaman, A. André, F. Massou, M. Fleischhauer, A. S. Zibrov, and M. D. Lukin, Electromagnetically induced transparency with tunable single-photon pulses, Nature **438**, 837 (2005).

[10] A. V. Gorshkov, A. André, M. Fleischhauer, A. S. Sørensen, and M. D. Lukin, Universal Approach to Optimal Photon Storage in Atomic Media, Phys. Rev. Lett. **98**, 123601 (2007).

[11] I. Novikova, R. L. Walsworth, and Y. Xiao, Electromagnetically induced transparency-based slow and stored light in warm atoms, Laser Photon. Rev. **6**, 333 (2012).

[12] A. S. Zibrov, A. B. Matsko, O. Kocharovskaya, Y. V. Rostovtsev, G. R. Welch, and M. O. Scully, Transporting and Time Reversing Light via Atomic Coherence, Phys. Rev. Lett. **88**, 103601 (2002).

[13] A. Raczyński and J. Zaremba, Controlled light storage in a double lambda system, Opt. Commun. **209**, 149 (2002).

[14] A. Raczyński and J. Zaremba, Electromagnetically induced transparency and storing of a pair of pulses of light, Phys. Rev. A **69**, 043801 (2004).

[15] X.-J. Liu, H. Jing, and M.-L. Ge, Quantum memory process with a four-level atomic ensemble, Eur. Phys. J. D **40**, 297 (2006).

[16] A. Eilam, A. D. Wilson-Gordon, and H. Friedmann, Slow and stored light in an amplifying double-Λ system, Opt. Lett. **33**, 1605 (2008).

[17] P. K. Vudyasetu, R. M. Camacho, and J. C. Howell, Storage and Retrieval of Multimode Transverse Images in Hot Atomic Rubidium Vapor, Phys. Rev. Lett. **100**, 123903 (2008).

[18] R. M. Camacho, P. K. Vudyasetu, and J. C. Howell, Four-wave-mixing stopped light in hot atomic rubidium vapour, Nat. Photon. **3**, 103 (2009).

[19] N. B. Phillips, A. V. Gorshkov, and I. Novikova, Light storage in an optically thick atomic ensemble under conditions of electromagnetically induced transparency and four-wave mixing, Phys. Rev. A **83**, 063823 (2011).

[20] D. Viscor, V. Ahufinger, J. Mompart, A. Zavatta, G. C. La Rocca, and M. Artoni, Two-color quantum memory in double-Λ media, Phys. Rev. A **86**, 053827 (2012).

[21] J. Wu, Y. Liu, D.-S. Ding, Z.-Y. Zhou, B.-S. Shi, and G.-C. Guo, Light storage based on four-wave mixing and electromagnetically induced transparency in cold atoms, Phys. Rev. A **87**, 013845 (2013).

[22] K. Zhang, J. Guo, L. Q. Chen, C. Yuan, Z. Y. Ou, and W. Zhang, Suppression of the four-wave-mixing background noise in a quantum memory retrieval process by channel blocking, Phys. Rev. A **90**, 033823 (2014).

[23] N. Lauk, C. O'Brien, and M. Fleischhauer, Fidelity of photon propagation in electromagnetically induced transparency in the presence of four-wave mixing, Phys. Rev. A **88**, 013823 (2013).

[24] As in Refs. [19,21], here we assume that the Stokes field is taken as a seeded idler that is input along with the probe field.

[25] Here ω is the deviation (sideband) of the center frequency of the probe and Stokes pulses, resulted from the coupling between the light fields and the atoms. Thus, the frequencies of the probe and Stokes fields are given by $\omega_p + \omega$ and $\omega_s + \omega$, respectively; the case $\omega = 0$ corresponds to the central frequency of both the probe and Stokes fields.

[26] Z. Liu, Y. Chen, Y. Chen, H. Lo, P. Tsai, Ite A. Yu, Y. Chen, and Y. Chen, Large Cross-Phase Modulations at the Few-Photon Level, Phys. Rev. Lett. **117**, 203601 (2016).

[27] Slow light and fast light refer to situations in which the group velocity is subluminal (i.e., $V_g \ll c$) and superluminal (i.e., $V_g > c$ or negative), respectively. See P. W. Milonni, *Fast Light, Slow Light and Left-handed Light* (IOP Publishing, Bristol, UK, 2005).

[28] A detailed discussion on how to realize condition (7) and related experimental consideration will be given elsewhere.

[29] Here we consider only the simple case, where the two control fields are switched off and on simultaneously.

[30] I. Novikova, N. B. Phillips, and A. V. Gorshkov, Optimal light storage with full pulse-shape control, Phys. Rev. A **78**, 021802(R) (2008).

[31] Y. Wu and L. Deng, Ultraslow Optical Solitons in a Cold Four-State Medium, Phys. Rev. Lett. **93**, 143904 (2004).

[32] G. Huang, L. Deng, and M. G. Payne, Dynamics of ultraslow optical solitons in a cold three-state atomic system, Phys. Rev. E **72**, 016617 (2005).

[33] Y. Chen, Z. Bai, and G. Huang, Ultraslow optical solitons and their storage and retrieval in an ultracold ladder-type atomic system, Phys. Rev. A **89**, 023835 (2014).

[34] Y. Chen, Z. Chen, and G. Huang, Storage and retrieval of vector optical solitons via double electromagnetically induced transparency, Phys. Rev. A **91**, 023820 (2015).

[35] Small radiations on edges of both pulses are observed for long-distance propagation, which are due to the high-order dispersion and high-order nonlinearity not considered in our analytical approach.

[36] R. W. Boyd, *Nonlinear Optics*, 3rd ed. (Academic Press, New York, 2008).